Energy &
Environmental Science

RSC Publishing

COMMUNICATION

View Article Online
View Journal | View Issue

CO_2/N_2 separations with mixed-matrix membranes containing Mg_2(dobdc) nanocrystals†

Cite this: *Energy Environ. Sci.*, 2013, **6**, 3565

Received 16th July 2013
Accepted 3rd September 2013

DOI: 10.1039/c3ee42394h

www.rsc.org/ees

Tae-Hyun Bae and Jeffrey R. Long*

Nanocrystals of M_2(dobdc) (M = Mg, Ni, Zn; dobdc^{4-} = 1,4-dioxido-2,5-benzenedicarboxylate), also known as M-MOF-74 or CPO-27-M, with diameters of ~100 nm or less were synthesized using a room-temperature reaction of 2 h duration. Adsorption data collected for CO_2 and N_2 show slightly lower surface areas but similar adsorption selectivites relative to the bulk materials. High-quality mixed-matrix membranes containing Mg_2(dobdc) nanocrystals were fabricated using three different polymers for testing under conditions relevant to the removal of CO_2 from flue gas. Significant enhancements in CO_2 permeability and CO_2/N_2 selectivity over a pure polymer membrane were observed when a glassy polyimide was employed as the matrix, while membranes made with rubbery polymers showed decreased permeabilities, presumably due to the plugging of Mg_2(dobdc) pores by polymer chains having a high mobility at room temperature.

Broader context

The development of energy-efficient CO_2 separation methods is critical for many energy and environmental technologies, including CO_2 capture, natural gas treatment, and hydrogen purification. Although membrane-based separations have been considered as a promising technology, the performance of current membrane materials should be improved further for industrial applications. One way to improve the performance of a polymeric membrane, which is also technically viable, is *via* incorporation of nanocrystals of a functional porous material, such as zeolite or metal–organic framework. In this work, mixed-matrix membranes containing nanocrystals of Mg_2(dobdc), a metal–organic framework exhibiting exceptional CO_2 adsorption properties, were fabricated and tested for CO_2/N_2 separation performance under dry flue gas conditions.

Metal–organic frameworks are porous crystalline materials composed of metal ions or clusters connected by organic linkers through strong chemical bonds.[1] Owing to their large surface areas and adjustable surface functionality, these compounds are currently under intense investigation for a variety of applications, including gas storage,[2–4] molecular separations,[5–7] sensing,[8] and catalysis.[9,10] In particular, they are of potential utility for gas separations in many energy and environmental technologies. So far, the majority of gas separation studies of metal–organic frameworks have focused on adsorptive separations.[5–7] However, membranes formed from these materials can also have excellent separation performance, due to the selective adsorption/transport of the target component in the feed mixture through the pore channels.[11] Although a number of studies on continuous films of metal–organic frameworks have been reported, their separation performance is often unsatisfactory, presumably owing to defects in the membranes, such as cracks and inter-crystal gaps, that permit the non-selective bypass of molecules.[7,11,12] In addition, it may be challenging to fabricate pure metal–organic framework membranes with large surface area that can be applied to industrial-scale separations.

A technically viable alternative is incorporating metal–organic framework particles into polymer membranes, since one could then combine the high separation performance of the porous frameworks with good processibility and mechanical stability of polymers.[7,13,14] While zeolites have been a mainstay for fabrication of such mixed-matrix membranes, utilizing metal–organic frameworks as fillers for improving the separation performance of polymer membranes has attracted much recent interest.[13] Especially, incorporating CO_2 selective framework adsorbents into polymer membranes is highly attractive due to the wide range of applications, including carbon dioxide capture, natural gas treatment, and hydrogen purification.

Numerous metal–organic frameworks exhibiting exceptional CO_2 separation properties have been synthesized.[7,15] In particular, Mg_2(dobdc) (dobdc^{4-} = 1,4-dioxido-2,5-benzenedicarboxylate; Mg-MOF-74, CPO-27-Mg), a framework in which the surfaces are decorated with a high concentration of

---

Department of Chemistry, University of California, Berkeley and Materials Sciences Division, Lawrence Berkeley National Laboratory, Berkeley, CA 94720, USA. E-mail: jrlong@berkeley.edu

† Electronic supplementary information (ESI) available: Experimental details, characterization of metal–organic frameworks, fitting parameters and calculations. See DOI: 10.1039/c3ee42394h

coordinatively unsaturated metal sites, has proven to be outstanding for the separation of CO_2 from N_2 or H_2 in adsorptive processes.[16,17] A computational study further indicated that a Mg_2(dobdc) membrane could have a high CO_2 kinetic separation performance for mixtures with H_2 or N_2, owing to selective adsorption and transport of the CO_2 molecules *via* the open metal sites located along the pore walls.[18] Moreover, Mg_2(dobdc) was predicted to have an extremely high CO_2 permeability as compared to most polymer and zeolite membranes, a very desireable property for application in post-combustion CO_2 capture from coal flue gas, for which the CO_2 feed gas pressure is as low as ~0.15 bar.[19]

In this work, we have developed a facile synthesis of M_2(dobdc) (M = Mg, Ni, Zn) nanocrystals displaying high porosities and uniform size distributions. After studying the CO_2/N_2 adsorption properties of the nanocrystals, mixed-matrix membranes were fabricated using the best performing metal–organic framework and various polymers were tested for potential application in post-combustion CO_2 capture.

Well-defined spherical Mg_2(dobdc) nanocrystals with diameters of ~100 nm were successfully synthesized at room temperature by carrying out the metal–organic framework assembly reaction in the presence of the organic base triethylamine. Fig. 1a shows the morphology of the resulting nanocrystals. Although several methodologies for the preparation of nanocrystals of metal–organic frameworks such as MOF-5 and various zeolitic imidazolate frameworks (ZIFs) have been reported,[20–23] to the best of our knowledge, well-defined nanocrystals of a M_2(dobdc) compound have not previously been generated. The reaction time of 2 h is much shorter than the conventional time of 20 h that gives rise to larger crystals with a broad size distribution (see Fig. S2 in the ESI†). The structure of the nanocrystals was confirmed by collecting a powder X-ray diffraction pattern (Fig. 1d), wherein significant peak broadening, as compared to the peak widths of solvothermally synthesized crystals, arises due to the smaller crystallites (Fig. S3†). Note that the size of crystallites estimated by the Scherrer equation was about 15 nm (see ESI† for calculation method). An N_2 adsorption isotherm measured at 77 K showed that the Mg_2(dobdc) nanocrystals have a high microporosity (Fig. S4†), with Langmuir and BET surface areas calculated as 1820 and 1380 $m^2\ g^{-1}$, respectively. For comparison, the values observed for the bulk material are 1905 and 1495 $m^2\ g^{-1}$, respectively.[16]

The methodology developed for Mg_2(dobdc) nanocrystal synthesis can be generalized to synthesis of the isostructural metal–organic frameworks containing various metal ions. As shown in Fig. 1b and c, nanocrystals of Ni_2(dobdc) and Zn_2(dobdc) formed with significantly smaller diameters of ~20 and ~30 nm, respectively. The framework structures were confirmed by collecting powder X-ray diffraction data, as shown in Fig. 1d.

Fig. 2 shows CO_2 and N_2 adsorption isotherms of the M_2(dobdc) nanocrystals measured at 25 °C. Similar to the differences reported previously for the bulk materials,[16] the Mg_2(dobdc) nanocrystals exhibit an excellent CO_2 adsorption capacity compared to the Zn- and Ni_2(dobdc) samples, especially at low CO_2 partial pressure. This is consistent with the expected strong interaction between the coordinatively unsaturated Mg^{2+} sites within the pores of the framework and the CO_2 molecules. The N_2 uptake in the Mg_2(dobdc) nanocrystals was also higher than for the other metal–organic frameworks. The CO_2 and N_2 adsorption data were fit with dual-site (DSL) and single-site Langmuir (SSL) models, respectively, as described in our previous work.[24] As depicted in Fig. 2, these models accurately described the CO_2 and N_2 adsorption isotherms for all of the samples (see ESI† for curve fitting parameters). Using these mathematical descriptions, Henry's coefficients, k_H, were calculated to quantify the gas adsorption properties. The CO_2/N_2 adsorption selectivities, here defined as the ratio of Henry's coefficients for CO_2 and N_2, were then estimated (see Table S3†). The Mg_2(dobdc) nanocrystals showed

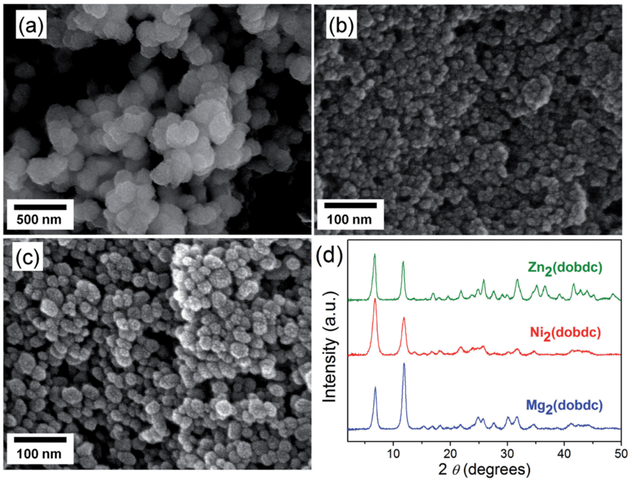

Fig. 1 SEM images of (a) Mg-, (b) Ni- and (c) Zn_2(dobdc) nanocrystals. (d) Powder X-ray diffraction patterns for the nanocrystalline samples.

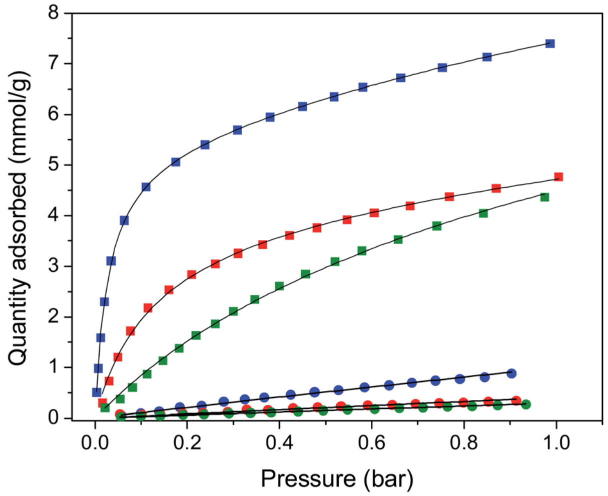

Fig. 2 Pure component CO_2 (squares) and N_2 (circles) adsorptions on Mg- (blue), Ni- (red) and Zn_2(dobdc) (green) nanocrystals measured at 25 °C. Solid lines correspond to fits to the CO_2 and N_2 data employing dual-site and single-site Langmuir models, respectively.

significantly higher Henry's coefficient for CO_2 adsorption (197 mmol g^{-1} bar^{-1}) compared to those for Ni- (35.0 mmol g^{-1} bar^{-1}) and Zn_2(dobdc) (9.60 mmol g^{-1} bar^{-1}) nanocrystals. The resulting CO_2/N_2 adsorption selectivity of 184 for the Mg_2(dobdc) sample was higher than for the other two materials. These results indicate that the Mg_2(dobdc) nanocrystals are clearly the most promising samples for use in attempting to enhance the CO_2/N_2 separation performance of polymer membranes.

Mixed-matrix membranes incorporating the Mg_2(dobdc) nanocrystals were fabricated using three different polymer matrices: two rubbery polymers and a glassy polymer. As shown in Fig. 3a and b, high-quality membranes containing no visible defects were obtained when polydimethylsiloxane (PDMS) was employed as the polymer matrix. Since the metal–organic framework nanocrystals were well dispersed in the organic solvent (here, toluene), they also distributed uniformly in the resultant membrane. In contrast, Mg_2(dobdc) nanocrystals were dispersed in neat monomers for forming membranes with cross-linked polyethylene oxide (XLPEO),[25,26] such that the casting solution became highly viscous even with 10 wt% filler loading. As a result, the Mg_2(dobdc) nanocrystals formed clusters in the polymer matrix, as evident in Fig. 3c and d, although no defects were apparent at the Mg_2(dobdc)/polymer interfaces. While, a "sieve in a cage" morphology is frequently observed in zeolite/glassy polymer composite membranes due to the poor compatibility between the two phases,[27–30] the Mg_2(dobdc) nanocrystals were found to be uniformly distributed in a glassy polyimide (PI = 6FDA-TMPDA where 6FDA = 2,2′ bis(3,4′-dicarboxyphenyl)hexafluoropropane dianhydride and TMPDA = 2,4,6-trimethyl-1,3-phenylenediamine),[31] without forming gaps at the filler/polymer interfaces (see Fig. 3e and f). This result strongly suggests that Mg_2(dobdc) nanocrystals can be used in fabricating composite films with glassy polymers without any additional efforts at making the two phases compatible. Similar observations have been made previously for sub-micrometer-sized metal–organic framework crystals.[20,21,32]

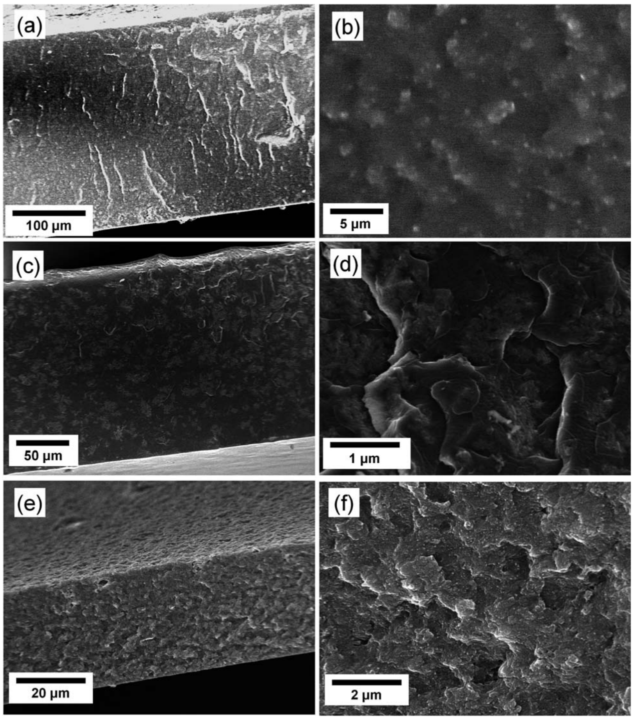

Fig. 3 SEM images of cross-sections of mixed-matrix membranes containing Mg_2(dobdc) nanocrystals. (a) and (b) 20 wt% Mg_2(dobdc) in PDMS; (c) and (d) 10 wt% Mg_2(dobdc) in XLPEO; (e) and (f) 10 wt% Mg_2(dobdc) in PI.

Pure component CO_2 and N_2 permeation properties for the three types of membranes are shown in Fig. 4. For composite membranes based upon the rubbery polymers PDMS and XLPEO, the CO_2 permeabilities unexpectedly decreased compared to those of pure polymer membranes, although CO_2/N_2 selectivities were slightly improved. Note that the theoretical study[18] predicted a significantly higher CO_2 permeability for Mg_2(dobdc) than is known for the pure polymers, due to the well-defined one-dimensional channels with a diameter of slightly greater than 1 nm. To probe the origin of the unexpected reduction in permeability, the CO_2 adsorption properties of the pure and composite films were measured. As shown in Fig. 5a and b, the composite membranes exhibit improved CO_2 adsorption properties compared to the pure polymers. However, the amounts of CO_2 uptake in the composite membranes are far lower than the calculated assuming the pores in all of the Mg_2(dobdc) nanocrystals in the membrane are available for CO_2 adsorption. This is presumably due to plugging of the pores by the flexible polymer chains, which have a small width compared to the channel diameter in the metal–organic framework. It should be noted that all possible contamination sources were removed from the membranes. The activated Mg_2(dobdc) nanocrystals were not exposed to air or moisture during membrane fabrication. Furthermore, prior to gas permeation and gas adsorption measurements, the membranes were heated at 180 °C under N_2 flow for one day to remove any residual solvent or water. Furthermore, X-ray diffraction measurements

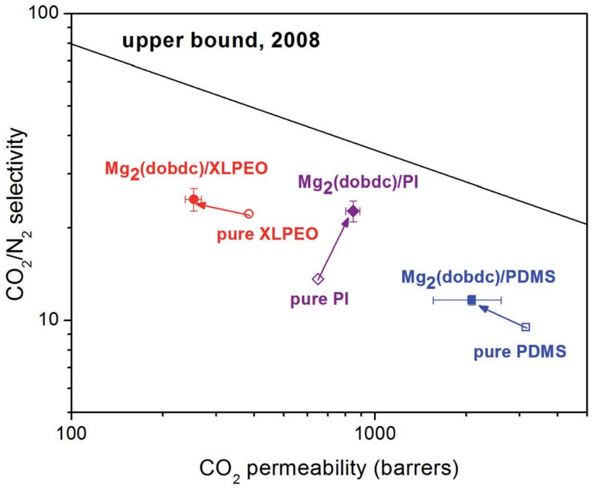

Fig. 4 Pure component CO_2 and N_2 permeation properties of membranes measured at 2 bar upstream pressure and 25 °C (see Table S4† for the precise values). The Mg_2(dobdc) loadings in composite membranes are 20, 10, and 10 wt % for PDMS, XLPEO and PI, respectively. The solid line represents the upper bound limit for polymeric membranes established in 2008.[33]

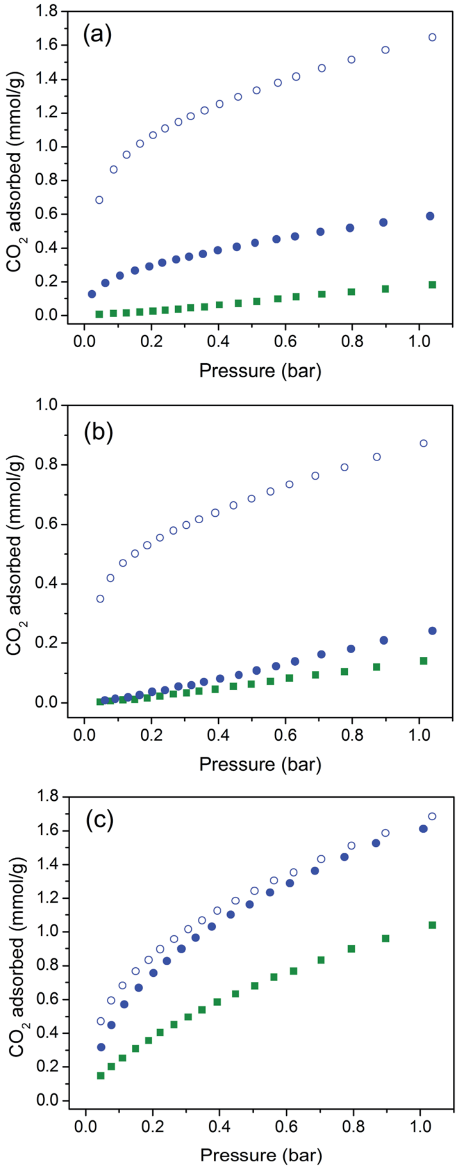

Fig. 5 CO_2 adsorption properties of pure polymer (green square) and mixed-matrix membranes (blue circle) measured at 25 °C. Hollow circles are the theoretical CO_2 uptake of mixed-matrix membranes when all metal–organic frameworks in membranes are available for CO_2 adsorption. Mg_2(dobdc) loadings are 20, 10 and 10 wt% for (a) PDMS, (b) XLPEO and (c) PI, respectively.

showed that the crystallinity of the Mg_2(bobdc) nanocrystals was retained in the mixed-matrix membranes, as shown in Fig. S4.†

In contrast, the mixed-matrix membrane based upon the glassy PI polymer, which possesses rigid aromatic and imide rings in the backbone, showed enhancement compared to a pure polymer membrane in both the CO_2 permeability (from 650 to 850 barrers) and CO_2/N_2 selectivity (from 14 to 23). As a result, the performance of the composite membrane is located in a position close to the Robeson upper bound established in 2008 (Fig. 4). Consistently, as shown in Fig. 5c, CO_2 adsorption in the PI mixed-matrix membrane is higher than for in the pure PI membrane. Furthermore, in contrast to the observations for the rubbery polymers, the amount of CO_2 uptake is much closer to the theoretical prediction, indicating most pores of the Mg_2(dobdc) nanocrystals embedded within the PI matrix are accessible to the permeating gas. Detailed analysis of CO_2 adsorption and permeation results revealed that the CO_2 solubility in the PI membrane dramatically increased upon incorporation of the Mg_2(dobdc) nanocrystals, while no significant change in CO_2 diffusivity was observed (see Table S5 in the ESI†). In contrast, CO_2 diffusivity significantly decreased in mixed-matrix membranes based upon rubbery polymers, presumably due to plugging of the outer pore windows of the Mg_2(dobdc) nanocrystals by the polymer chains. To the best of our knowledge, pore plugging by rubbery polymer chains has not been observed in mixed-matrix membranes containing zeolites, which typically have pore windows far smaller than 1 nm. Thus, the findings of this study indicate that the molecular structure and mobility of the polymer chains and the pore dimension of fillers can be important factors in the design of mixed-matrix membranes incorporating adsorbents with large pore windows.

The foregoing results demonstrate that the CO_2 separation performance of polymer membrane can be significantly enhanced by incorporating Mg_2(dobdc) nanocrystals within a glassy polymer. The overall CO_2/N_2 separation characteristics of the 10 wt% Mg_2(dobdc)/PI membrane prepared in this work are arguably the best yet reported for any metal–organic framework mixed-matrix membrane (see Fig. S6† (ref. 7)). In particular, it offers improvements in both selectivity and permeability over a high-performance membrane wherein a small pore metal–organic framework, ZIF-90, was incorporated to enhance diffusion selectivity.[21] Future efforts will be devoted to fabricating asymmetric Mg_2(dobdc)/PI membranes in which a thin skin layer containing a large weight fraction of metal–organic framework nanocrystals is supported by the porous polymer layer. In addition, mixed gas permeation properties will be studied under conditions relevant to post-combustion CO_2 capture.

Acknowledgements

This work was supported by the Assistant Secretary for Fossil Energy of the U.S. Department of Energy under Contract no. DE-AC02-05CH11231.

Notes and references

1 G. Ferey, *Chem. Soc. Rev.*, 2008, **37**, 191–214.
2 L. J. Murray, M. Dinca and J. R. Long, *Chem. Soc. Rev.*, 2009, **38**, 1294–1314.
3 K. Konstas, T. Osl, Y. Yang, M. Batten, N. Burke, A. J. Hill and M. R. Hill, *J. Mater. Chem.*, 2012, **22**, 16698–16708.
4 M. P. Suh, H. J. Park, T. K. Prasad and D.-W. Lim, *Chem. Rev.*, 2011, **112**, 782–835.
5 J. R. Li, R. J. Kuppler and H. C. Zhou, *Chem. Soc. Rev.*, 2009, **38**, 1477–1504.
6 J. R. Li, J. Sculley and H. C. Zhou, *Chem. Rev.*, 2012, **112**, 869–932.

7 K. Sumida, D. L. Rogow, J. A. Mason, T. M. McDonald, E. D. Bloch, Z. R. Herm, T. H. Bae and J. R. Long, *Chem. Rev.*, 2012, **112**, 724–781.

8 L. E. Kreno, K. Leong, O. K. Farha, M. Allendorf, R. P. Van Duyne and J. T. Hupp, *Chem. Rev.*, 2011, **112**, 1105–1125.

9 J. Lee, O. K. Farha, J. Roberts, K. A. Scheidt, S. T. Nguyen and J. T. Hupp, *Chem. Soc. Rev.*, 2009, **38**, 1450–1459.

10 M. Yoon, R. Srirambalaji and K. Kim, *Chem. Rev.*, 2011, **112**, 1196–1231.

11 J. Gascon and F. Kapteijn, *Angew. Chem., Int. Ed.*, 2010, **49**, 1530–1532.

12 M. Shah, M. C. McCarthy, S. Sachdeva, A. K. Lee and H.-K. Jeong, *Ind. Eng. Chem. Res.*, 2011, **51**, 2179–2199.

13 H. B. Tanh Jeazet, C. Staudt and C. Janiak, *Dalton Trans.*, 2012, **41**, 14003–14027.

14 T.-S. Chung, L. Y. Jiang, Y. Li and S. Kulprathipanja, *Prog. Polym. Sci.*, 2007, **32**, 483–507.

15 D. M. D'Alessandro, B. Smit and J. R. Long, *Angew. Chem., Int. Ed.*, 2010, **49**, 6058–6082.

16 S. R. Caskey, A. G. Wong-Foy and A. J. Matzger, *J. Am. Chem. Soc.*, 2008, **130**, 10870–10871.

17 J. A. Mason, K. Sumida, Z. R. Herm, R. Krishna and J. R. Long, *Energy Environ. Sci.*, 2011, **4**, 3030–3040.

18 R. Krishna and J. M. van Baten, *J. Membr. Sci.*, 2011, **377**, 249–260.

19 E. J. Granite and H. W. Pennline, *Ind. Eng. Chem. Res.*, 2002, **41**, 5470–5476.

20 E. V. Perez, K. J. Balkus Jr, J. P. Ferraris and I. H. Musselman, *J. Membr. Sci.*, 2009, **328**, 165–173.

21 T.-H. Bae, J. S. Lee, W. Qiu, W. J. Koros, C. W. Jones and S. Nair, *Angew. Chem., Int. Ed.*, 2010, **49**, 9863–9866.

22 Y. Pan, Y. Liu, G. Zeng, L. Zhao and Z. Lai, *Chem. Commun.*, 2011, **47**, 2071–2073.

23 J. Cravillon, S. Münzer, S.-J. Lohmeier, A. Feldhoff, K. Huber and M. Wiebcke, *Chem. Mater.*, 2009, **21**, 1410–1412.

24 T.-H. Bae, M. R. Hudson, J. A. Mason, W. L. Queen, J. J. Dutton, K. Sumida, K. J. Micklash, S. S. Kaye, C. M. Brown and J. R. Long, *Energy Environ. Sci.*, 2013, **6**, 128–138.

25 H. Lin, E. Van Wagner, B. D. Freeman, L. G. Toy and R. P. Gupta, *Science*, 2006, **311**, 639–642.

26 H. Lin, E. Van Wagner, R. Raharjo, B. D. Freeman and I. Roman, *Adv. Mater.*, 2006, **18**, 39–44.

27 T. H. Bae, J. Q. Liu, J. S. Lee, W. J. Koros, C. W. Jones and S. Nair, *J. Am. Chem. Soc.*, 2009, **131**, 14662–14663.

28 T. H. Bae, J. Q. Liu, J. A. Thompson, W. J. Koros, C. W. Jones and S. Nair, *Microporous Mesoporous Mater.*, 2011, **139**, 120–129.

29 M. E. Lydon, K. A. Unocic, T.-H. Bae, C. W. Jones and S. Nair, *J. Phys. Chem. C*, 2012, **116**, 9636–9645.

30 J. Liu, T.-H. Bae, W. Qiu, S. Husain, S. Nair, C. W. Jones, R. R. Chance and W. J. Koros, *J. Membr. Sci.*, 2009, **343**, 157–163.

31 L. Wang, Y. Cao, M. Zhou, S. J. Zhou and Q. Yuan, *J. Membr. Sci.*, 2007, **305**, 338–346.

32 Y. Zhang, I. H. Musselman, J. P. Ferraris and K. J. Balkus Jr, *J. Membr. Sci.*, 2008, **313**, 170–181.

33 L. M. Robeson, *J. Membr. Sci.*, 2008, **320**, 390–400.